Chaos
An Interdisciplinary Journal of Nonlinear Science

RESEARCH ARTICLE | JULY 07 2023

A physical understanding and quantification for the regulation of orexin on sleep FREE

Special Collection: Nonlinear dynamics, synchronization and networks: Dedicated to Jürgen Kurths' 70th birthday

Chenggui Yao ; Fei Xu; Xiangdong Tang; Wei Zou ; Dongping Yang ; Jianwei Shuai

Chaos 33, 073119 (2023)
https://doi.org/10.1063/5.0156090

A physical understanding and quantification for the regulation of orexin on sleep

Cite as: Chaos 33, 073119 (2023); doi: 10.1063/5.0156090
Submitted: 26 April 2023 · Accepted: 20 June 2023 ·
Published Online: 7 July 2023

Chenggui Yao,[1,2,3] Fei Xu,[4] Xiangdong Tang,[5] Wei Zou,[6,a)] Dongping Yang,[2,a)] and Jianwei Shuai[7]

AFFILIATIONS

[1]College of Data Science, Jiaxing University, Jiaxing 314000, China
[2]Research Center for Augmented Intelligence, Research Institute of Artificial Intelligence, Zhejiang Lab, Hangzhou, Zhejiang 311101, China
[3]Wenzhou Key Laboratory of Biophysics, Wenzhou Institute, University of Chinese Academy of Sciences, Wenzhou 325000, China
[4]Department of Physics, Xiamen University, Xiamen 361005, People's Republic of China
[5]Sleep Medicine Center, Mental Health Center, Department of Respiratory and Critical Care Medicine, State Key Laboratory of Biotherapy, West China Hospital, Sichuan University, Chengdu 610041, China
[6]School of Mathematical Sciences, South China Normal University, Guangzhou 510631, People's Republic of China
[7]Oujiang Laboratory (Zhejiang Lab for Regenerative Medicine, Vision and Brain Health), and Wenzhou Institute, University of Chinese Academy of Sciences, Wenzhou, Zhejiang 325001, China

Note: This paper is part of the Focus Issue on Nonlinear dynamics, synchronization and networks: Dedicated to Juergen Kurths' 70th birthday.

[a)]**Authors to whom correspondence should be addressed:** weizou83@gmail.com and dpyang@zhejianglab.com

ABSTRACT

The orexinergic neurons located in the lateral hypothalamus play a vital role in maintaining wakefulness and regulating sleep stability. Previous research has demonstrated that the absence of orexin (Orx) can trigger narcolepsy, a condition characterized by frequent shifts between wakefulness and sleep. However, the specific mechanisms and temporal patterns through which Orx regulates wakefulness/sleep are not fully understood. In this study, we developed a new model that combines the classical Phillips–Robinson sleep model with the Orx network. Our model incorporates a recently discovered indirect inhibition of Orx on sleep-promoting neurons in the ventrolateral preoptic nucleus. By integrating appropriate physiological parameters, our model successfully replicated the dynamic behavior of normal sleep under the influence of circadian drive and homeostatic processes. Furthermore, our results from the new sleep model unveiled two distinct effects of Orx: excitation of wake-active neurons and inhibition of sleep-active neurons. The excitation effect helps to sustain wakefulness, while the inhibition effect contributes to arousal, consistent with experimental findings [De Luca *et al.*, Nat. Commun. **13**, 4163 (2022)]. Moreover, we utilized the theory of potential landscapes to investigate the physical mechanisms underlying the frequent transitions observed in narcolepsy. The topography of the underlying landscape delineated the brain's capacity to transition between different states. Additionally, we examined the impact of Orx on barrier height. Our analysis demonstrated that a reduced level of Orx led to a bistable state with an extremely low threshold, contributing to the development of narcoleptic sleep disorder.

The investigation of sleep dynamics has attracted considerable interest among researchers owing to its crucial function in maintaining normal development, stabilizing various metabolic functions, and improving the body's immunity. Notably, comprehending the mechanisms underlying orexin-deficit narcolepsy is pivotal for advancing the development of effective therapies for sleep disorders, and sleep dynamics are instrumental in achieving this goal. In this study, we developed a mathematical model that incorporated the excitation of Orx on wake-active monoaminergic neurons (MA) and the inhibition of Orx on sleep-active ventrolateral preoptic neurons (VLPO). By utilizing this sleep model, we were able to replicate normal sleep with a 24-h circadian rhythm through circadian drive and homeostatic processes. Our analysis revealed the function of Orx excitation in sustaining wakefulness and the inhibitory effect of Orx on sleep-active neurons in promoting arousal. To elucidate the physical mechanisms

underlying frequent transitions in narcolepsy, we employed the theory of underlying landscape. Our investigation demonstrated that decreased levels of Orx resulted in a bistable state with a remarkably low threshold, offering a more lucid physical interpretation of how the loss of Orx leads to instability of the arousal state.

I. INTRODUCTION

Orexin is a neuropeptide that was independently discovered in 1998 by two research groups,[1,2] marking a notable breakthrough due to its involvement in a multitude of neurological processes, including sleep and wakefulness regulation.[3,4] The active orexinergic neurons located in the lateral hypothalamic area (Orx) exert a pivotal role in promoting arousal and maintaining wakefulness, and Orx's influence extends to other brain regions that control sleep, thus regulating the wake/sleep cycle.[5,6] In addition to sleep regulation, Orx has also been shown to impact appetite and energy metabolism. Previous research has demonstrated that Orx promotes feeding and increases energy expenditure, suggesting that it may be a target for developing anti-obesity drugs.[7–9] Researchers have also reported that the loss of Orx leads to narcolepsy, a disorder characterized by excessive daytime sleepiness and sudden attacks of sleep.[10–15] The loss of Orx in narcoleptic patients indicates that it plays a crucial role in regulating the wake/sleep cycle.[16,17]

Although the relationship between Orx and narcolepsy has been elaborated in detail,[10] and the action network and key neurological pathways of Orx have been gradually revealed,[3,4] the physical mechanisms responsible for how the loss of Orx can induce fragmented sleep in narcolepsy have yet to be fully elucidated.[18] Although Fulcher *et al.* have reported that orexin neurons play a role in stabilizing the wake/sleep switch,[19] the physical mechanism responsible for the frequent transition of narcolepsy has yet to be fully described. Furthermore, experimental findings indicate that Orx neurons indirectly inhibit sleep-promoting neurons in the ventrolateral preoptic nucleus (VLPO) and contribute to maintaining arousal.[20] Thus, a comparison of the roles of Orx on exciting MA and inhibiting VLPO is also necessary to fully understand the crucial factors involved in narcolepsy.

Sleep is not a static phenomenon; rather, it is highly dynamic. It arises due to the interaction between the 24-h master circadian pacemaker in the suprachiasmatic nucleus (SCN) of the hypothalamus, which is entrained to periodic photic input,[21] and a homeostatic process that increases during wakefulness and declines during sleep.[22] Experimental and theoretical studies have revealed the regulatory mechanism responsible for states of sleep and wakefulness.[23–26] For example, many studies have experimentally identified numerous brain regions spanning the hypothalamus, forebrain, midbrain, and hindbrain in regulating sleep and wakefulness. These include wake-active neurons that use monoaminergic neurotransmitters, such as the histaminergic tuberomammillary nucleus (TMN), the dopaminergic ventral tegmental area (VTA), the norepinephrinergic locus coeruleus (LC), and the serotoninergic dorsal raphe nucleus (DR),[27–29] as well as sleep-active neurons in the preoptic area (POA) of the hypothalamus, the parabrachial nucleus (PB) in the hindbrain, and the ventrolateral periaqueductal gray (vlPAG) in the midbrain.[30–32] Mutual inhibitions between the wake-active nuclei and sleep-active neurons give rise to switch-like dynamics between states of sleep and wakefulness,[30,31] contributing to the discrete separation of sleep and wakefulness states. Based on these switch dynamics, several physiological models, including key sleep-regulatory nuclei in the brainstem and hypothalamus, have been developed to understand the generation of the circadian rhythm. One classical model, the two-process model, combines the homeostatic process and circadian pacemaker into a theoretical model that can quantitatively describe the timing of sleep and wakefulness.[33]

The regulation of sleep is widely recognized as a complex process involving numerous factors and feedback loops. However, a mathematical model not only provides valuable insights into how these factors interact and contribute to the overall regulation of sleep but also offers a more precise and objective understanding of the dynamics of sleep. The Phillips–Robinson (PR) sleep model[24] is constructed based on the mutually inhibitory sleep-active ventrolateral preoptic nucleus (VLPO) and the wake-active monoaminergic (MA) group. This model exhibits flip-flop dynamics between sleep and wakefulness, driven by both homeostatic and circadian processes. While waking/sleep dynamics are known to be regulated by various processes,[34] the PR model can describe the dynamic mechanism of the wake/sleep system[24] and explain the rules governing the amount of sleep, including fragmented sleep,[19] differences in sleep patterns,[35] sleep deprivation effects,[25] caffeine effects and shift effects,[36] and micro-sleep.[26] Additionally, other theoretical models have been proposed to qualitatively explain many wake/sleep dynamical phenomena.[37–39]

In this study, we developed a sleep model capable of producing a circadian rhythm between wakefulness and sleep based on the PR model. We combined the PR model with the action network of Orx, considering the newly discovered indirect inhibition of Orx on VLPO.[20] Our study had four objectives: (i) to construct a two "flip-flop" model between wakefulness and sleep based on the average properties of large populations of neurons and their interactions; (ii) to illustrate the distinct roles of Orx on exciting MA and inhibiting VLPO; (iii) to identify the mechanisms underlying the regulatory effect of Orx on sleep; and (iv) to uncover the physical mechanism responsible for the narcolepsy induced by the loss of Orx using physical theory. Section II introduces relevant physiological models and two "flip-flop" models, with numerical results presented in Sec. III. Section IV provides relevant discussions and conclusions.

II. MODEL AND METHODS

A. Basic physiological elements of the model

In this research, the sleep model is developed with the regulation by Orx and modified from the existing model developed by Phillips and Robinson.[24] The original model incorporates interactions between two key neuronal populations (VLPO and MA) as well as circadian and homeostatic drives. In the new model, we consider mutually inhibitory interactions between Orx and VLPO, as well as the excitatory input of Orx on MA. Although the regulation of sleep involves a wide range of processes,[34] VLPO, MA, and Orx are known to play leading roles in this complex system.[21]

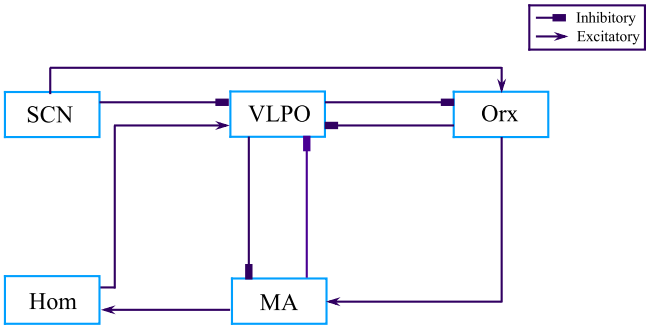

FIG. 1. Schematic of the flip-flop model of the wakefulness-sleep switch. The model incorporates the sleep-active ventrolateral preoptic area of the hypothalamus (VLPO), the wake-active monoaminergic brainstem nuclei (MA), and the orexinergic neurons of the lateral hypothalamic area (Orx), along with the circadian (C) drive in the suprachiasmatic nucleus (SCN) and the homeostatic (H) drive.

The basic elements of the model include wake-promoting neurons and sleep-promoting neurons. The flip-flop dynamics of sleep and wakefulness are believed to be caused by the mutual inhibition between wake-active MA and sleep-active VLPO neurons. The MA neuronal group, which utilizes monoaminergic neurotransmitters, can inhibit the VLPO, while the VLPO, with GABAergic projections, can feedback to inhibit the MA neuronal populations.[40,41] Orx regulates wakefulness and sleep through its excitatory input on the MA and its newly discovered indirect inhibition on the VLPO.[19,20] Furthermore, the dynamics of wakefulness and sleep are primarily controlled by the circadian (C) and homeostatic drive (H). The 24-h circadian signal originates from the suprachiasmatic nucleus of the hypothalamus (SCN), which is entrained by the light/dark cycle.[21] The VLPO receives an inhibitory circadian projection, while Orx receives an excitatory circadian projection, primarily via the dorsomedial nucleus of the hypothalamus (DMH) that receives the excitatory projection from SCN.[42,43] The homeostatic drive, which excites VLPO neurons,[44] increases during wakefulness and decreases during sleep.[22] A schematic depiction of this model, which includes the three basic elements mentioned above (circadian and homeostatic drive and neuronal interactions), is shown in Fig. 1.

B. Dynamical equations and neuronal interactions

Following the PR model, we also considered the average properties of neuronal populations and their interactions.[24,25] The dynamical equation for Orx was formulated as a neuronal population in the same manner as for the MA and VLPO. Building upon the basic elements and neuronal interactions described above, the equations governing the VLPO (v), MA (m), and Orx (x) populations can be given as follows:

$$\frac{\tau_m dV_m}{dt} = -V_m + \nu_{mv}Q_v + \nu_{mx}Q_x + D_m^{'} + \xi_m(t), \tag{1a}$$

$$\frac{\tau_v dV_v}{dt} = -V_v + \nu_{vm}Q_m + \nu_{vx}Q_x + D_v^{'} + \xi_v(t), \tag{1b}$$

$$\frac{\tau_x dV_x}{dt} = -V_x + \nu_{xv}Q_v + D_x^{'}, \tag{1c}$$

where the time constants, τ_j, control the rate at which the dynamics of V_j evolve via the decay rate of neuromodulator effects for $j = m, v, x$. V_j and Q_j for $j = m, v, x$ stand for mean cell-body potentials relative to resting ones and mean firing rating of MA-active, VLPO-active neurons, and orexinergic neurons, respectively. $\xi_j(t)$ for $j = m, v$ are an independent Gaussian white noise with $\langle \xi_j(t) \rangle = 0$ and $\langle \xi_i(t)\xi_j(t^{'}) \rangle = 2\sigma\delta_{ij}\delta(t - t^{'})$, where σ denotes the noise strength. Q_j is approximated as a sigmoidal function of V_j, for $(j = m, v, x)$, given as

$$Q_j = S(V_j) = \frac{Q_{max}}{1 + \exp\left(-(V_j - \theta)/\sigma^{'}\right)}, \tag{2}$$

where Q_{max} represents the maximum firing rate, θ is mean firing threshold, and $\sigma^{'}\pi/\sqrt{3}$ stands for standard deviation.[24,25] In Eq. (1), ν_{ij} for $(i, j = m, v, x, i \neq j)$ are the coefficients of neuronal interactions, whose sign determines the type of interaction. It can capture the inhibition (excitation) between three states by setting $\nu_{ij} < 0$ ($\nu_{ij} > 0$). $D_j^{'}$ for $j = m, v, x$ are the grouped drives from the two-process model.

C. Two-process model

In our model, two different drives are considered, including circadian (C) and homeostatic drive (H). The circadian drive is modeled by a sinusoidal function due to the entrainment of the light/dark cycle,[24]

$$C(t) = \sin(\omega_c t), \tag{3}$$

with $\omega_c = \frac{2\pi}{24}h^{-1}$. Without loss of generality, the amplitude is set to 1 as the actual amplitude is absorbed into the coefficients of interactions between populations and the circadian drive.

To model the homeostatic drive H, we used a nonlinear dynamical differential equation which depends on the state of arousal,[24]

$$\chi\frac{dH}{dt} = -H + \nu_{hm}\frac{Q_m^2}{\eta + Q_m^2}, \tag{4}$$

where χ is the timescale that describes the change of H. The constants η and ν_{hm} control dependence H on Q_m. To model the increase of homeostatic pressure during wake and its decrease during sleep, the coefficient ν_{hm} is set to be positive, i.e., $\nu_{hm} > 0$.

Further, the net drives to the neuronal populations via the circadian and homeostatic drives can be redefined as follows:

$$D_m = D_m^{'} = \nu_{mx}Q_x + A_m, \tag{5a}$$

$$D_v = \nu_{vx}Q_x + D_v^{'} = \nu_{vx}Q_x + \nu_{vc}C + \nu_{vh}H + A_v, \tag{5b}$$

$$D_x = D_x^{'} = \nu_{xc}C + A_x, \tag{5c}$$

where $\nu_{mx} > 0$ because Orx neurons excite wake-active populations;[19] $\nu_{vx} < 0$ because Orx neurons indirectly inhibit VLPO-active populations. $\nu_{xc} > 0$ and $\nu_{vc} < 0$ indicate that the Orx neurons and VLPO-active populations receive the excitatory and inhibitory inputs from the DMH, respectively. $\nu_{vh} > 0$ due to the

TABLE I. Parameter values.

	Param.	Value	Param.	Value	Param.	Value
	ν_{mv}	−1.80 mV s	ν_{mx}	0.30 mV s	ν_{vm}	−2.10 mV s
Connection strengths	ν_{vx}	−0.36 mV s	ν_{vc}	−0.20 mV s	ν_{vh}	1.00 mV s
	ν_{xv}	−0.50 mV s	ν_{xc}	0.60 mV s		
Time constants	τ_m	10 s	τ_v	10 s	τ_x	120 s
Constants drives	A_m	0.8 mV	A_v	−7.5 mV	A_x	1.0 mV
Homeostatic dynamics	ν_{hm}	17.0 mV s	η	2.3		
	Q_{max}	100 s^{-1}	θ	10 mV	$\sigma_\prime$	3 mV
Others parameters	σ	0.005 mV				

excitatory input from the homeostatic process. Constants, $A_{m,v,x}$, represent averaged inputs to each population from external sources, and all constant offsets of the circadian can be absorbed into the corresponding A_j. Our model was developed based on the original PR sleep model, while it brings many new parameters. All parameters are shown in in Table I. Our purpose for constructing the new model was to investigate the regulatory function of Orx on sleep; thus, we did not perform rigorous parameter constraints by fitting them to clinical datasets.

To integrate neuronal interactions and the two different drives, four ordinary differential equations were generated for the full model,

$$\frac{\tau_m dV_m}{dt} = -V_m + \nu_{mv}Q_v + \nu_{mx}Q_x + A_m + \xi_m(t), \tag{6a}$$

$$\frac{\tau_v dV_v}{dt} = -V_v + \nu_{vm}Q_m + \nu_{vx}Q_x + \nu_{vc}C + \nu_{vh}H + A_v + \xi_v(t), \tag{6b}$$

$$\frac{\tau_x dV_x}{dt} = -V_x + \nu_{xv}Q_v + \nu_{xc}C + A_x, \tag{6c}$$

$$\chi\frac{dH}{dt} = -H + \nu_{hm}\frac{Q_m^2}{\eta + Q_m^2}, \tag{6d}$$

where C is given in Eq. (3). Equation (6) is solved numerically by the standard fourth-order Runge–Kutta approach with a fixed time step $\Delta t = 0.01$ s.

III. RESULTS

A. Dynamics of sleep with different levels of orexin

In this section, we explore how the dynamics of normal sleep are regulated by different levels of Orx. Since Orx in our model is regarded as an excitatory input to the MA and an inhibitory action on VLPO, the level of Orx can be modeled by setting $\nu'_{mx} = r_1\nu_{mx}$ and $\nu'_{vx} = r_2\nu_{vx}$, with r_1 and r_2 representing the relative two effects of Orx, ν'_{mx} and ν'_{vx} as the controlling parameters, and ν_{mx} and ν_{vx} denoting the nominal interaction strengths. If the effects of Orx are excluded with $r_1 = r_2 = 0$, the model returns to the original PR model, except the change of the reduced magnitude of circadian input to VLPO ν_{vc}: $\nu_{vc} \in [-3.2, -2.7]$ mV in the original PR model,[25] while $\nu_{vc} = -0.2$ mV in our model. The distinction was initially proposed by Fulcher *et al.*[19] and highlighted the significant involvement of Orx in the circadian regulation of sleep.[45] It is supported by experimental findings that even in the presence of VLPO lesions, robust circadian rhythmicity in sleep-wake behavior is maintained.[46]

First, we consider the noise-free model with the combination of two drives, including an oscillatory circadian input C and a homeostatic drive H. Figure 2 shows a 1.5-day time series for Q_m, Q_v, and Q_x. From Fig. 2(a) with a sufficiently large level of Orx ($r_1 = r_2 = 1.0$), it is clear that during sleep, the value of Q_v is large and decreases during the night until the transition to wakefulness. Accordingly, the dynamics for normal sleep with approximately 15.9 h of wakefulness and 8.1 h of sleep were generated under appropriate parameters [Fig. 2(a_1)]. It is evident that there is an increase in homeostatic pressure during the period of wake and a dissipation of homeostatic pressure during sleep [plotted in green in Fig. 2(a_2)]. Furthermore, Orx is activated during wake and suppressed during sleep (the black line in Fig. 2).

When the level of Orx decreases to half that of normal sleep ($r_1 = r_2 = 0.5$), one can also find flip-flop dynamics of sleep and wakefulness. No significant difference compared to normal sleep can be found in the time series of Q_m and Q_v. However, upon closer inspection of the pattern in Fig. 2(b_1), we noticed a decrease in the amplitude of Q_m and Q_v, leading to an increase in the duration of sleep bouts due to reduced excitation of Orx on MA and inhibition on VLPO. From Fig. 2(b_2), it is evident that the homeostatic process and circadian drive performed their normal functions.

When the level of Orx is reduced to a quarter of that observed in normal sleep ($r_1 = r_2 = 0.25$), we observe the emergence of flip-flop dynamics between sleep and wakefulness, resulting from mutual inhibitory interactions. However, this abnormal transition between wakefulness and sleep deviates from the typical pattern. From the analysis of Fig. 2(c_1), it is evident that approximately 9 h of sleep per day are generated, with an additional 3 h of sleep occurring during the daytime, as observed in the time series for Q_v and C. This additional sleep during the daytime highlights the role of Orx in sustaining wakefulness. Furthermore, it can be noted that the amplitudes of Q_m and Q_v decrease as the level of Orx is reduced.

Finally, when Orx is completely removed from the model ($r_1 = r_2 = 0$), the simulated 36-h firing rate time series of the new model without Orx are plotted in Fig. 2(d_1). As shown, the circadian rhythm in the sleep process completely disappeared, and the

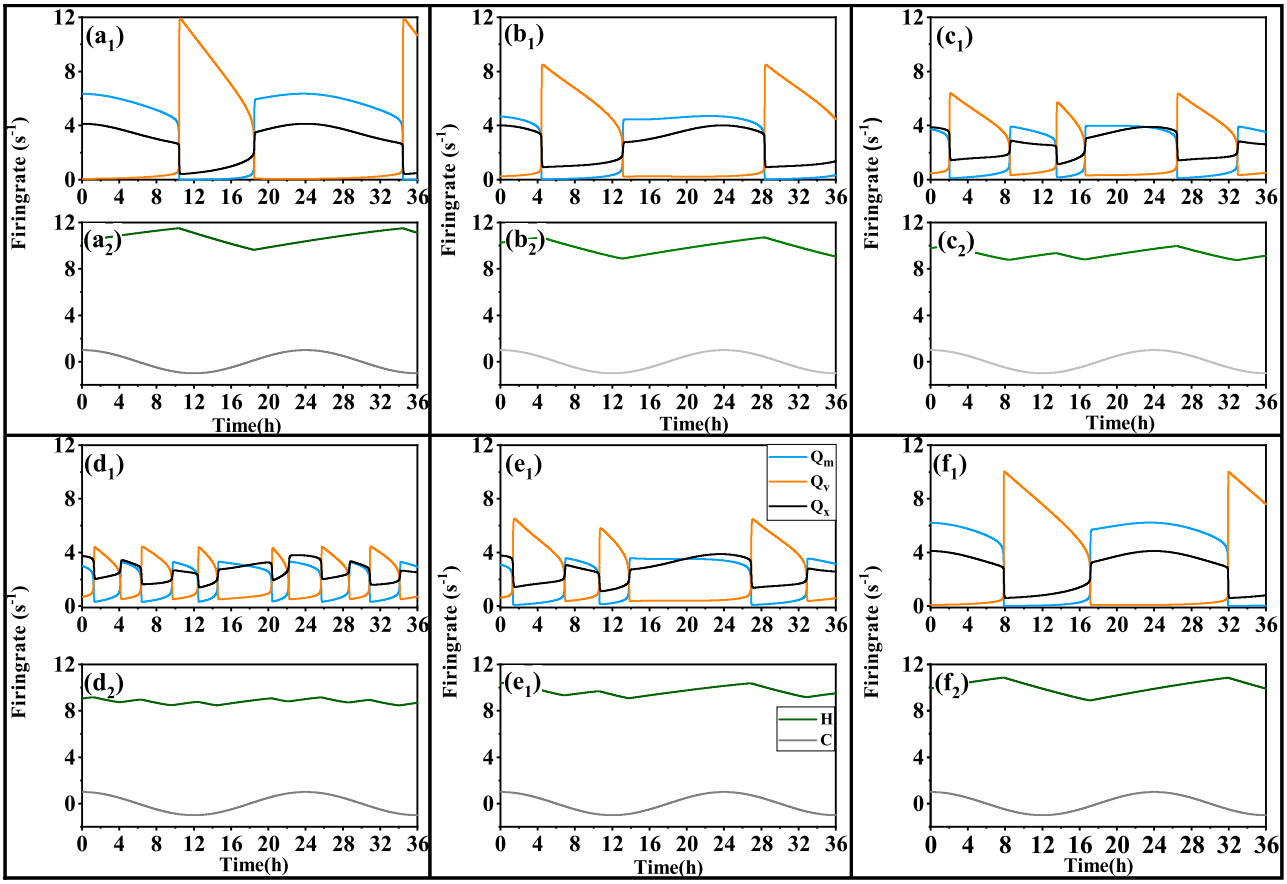

FIG. 2. (a_1)–(f_1) Firing rates Q_m (blue), Q_v (orange), and Q_x (black) for ($r_1 = 1.0, r_2 = 1.0$), ($r_1 = 0.5, r_2 = 0.5$), ($r_1 = 0.25, r_2 = 0.25$), ($r_1 = 0.0, r_2 = 0.0$), ($r_1 = 0.0, r_2 = 1.0$), and ($r_1 = 1.0, r_2 = 0.0$), respectively. The homeostatic process H [green, Eq. (5)] and the circadian drive C [gray, Eq. (7)] are shown in (a_2)–(f_2).

number of transitions between wakefulness and sleep per day significantly increased. Without Orx, it is almost impossible to maintain wakefulness, while sleep cannot be prolonged.

Regarding the comparison between the excitation of Orx on MA and the inhibition of Orx on VLPO, Figs. 2(e_1) and 2(f_1) show the time series of Q_m and Q_v with $r_1 = 0.0, r_2 = 1.0$ (without excitation) and $r_1 = 1.0, r_2 = 0.0$ (without inhibition), respectively. By comparing these two cases, we can identify abnormal wakefulness and a disorderly switch between wakefulness and sleep without the excitation of Orx on MA [Fig. 2(e_1)], indicating that excitatory effects play a role in maintaining wakefulness. What is important, we observed a similar progression of normal sleep with a bit longer sleep duration without the inhibition of Orx on MA [Fig. 2(f_1)], demonstrating the inhibitory effect of Orx on VLPO plays a role in awakening from sleep.

B. The effect of Orx on the hysteresis loop

In a previous study, Phillips and Robinson have reported that the normal wake/sleep dynamics arise from the hysteresis loop with changes in D_v, which is composed of the combination of the net oscillatory drives H and C, while the drive D_m remains constant.[24] By considering the excitation of Orx on MA and the inhibition of Orx on VLPO, the new model produces a trajectory resembling a loop through the (D_v, D_m) plane, as shown in Fig. 3(a). During normal sleep, when the system is in a wakeful state, Orx is active. Initially, D_m increases but then decreases due to the change of Q_x induced by C. In contrast, D_v increases due to the heightened activity of H and the weakened inhibition of Orx. This leads to a change in D_m and D_v that moves the system from the wake region, through the bistable region, and into the sleep region. When the brain is in a sleep state, Orx is inactive due to inhibition from VLPO. The value of D_m is small and increases with the increased activity of C. On the other hand, D_v decreases from a large value due to the reduced activity of the homeostatic sleep drive H. Eventually, the drive D_m reaches a sufficiently large value while D_v decreases to a small value, triggering a transition back to a wakeful state. Upon awakening from sleep, Orx activates the MA by increasing D_m and inhibits VLPO by reducing D_v, thereby preventing transitions back to sleep and maintaining wakefulness by consolidating periods of the wake. After the brain

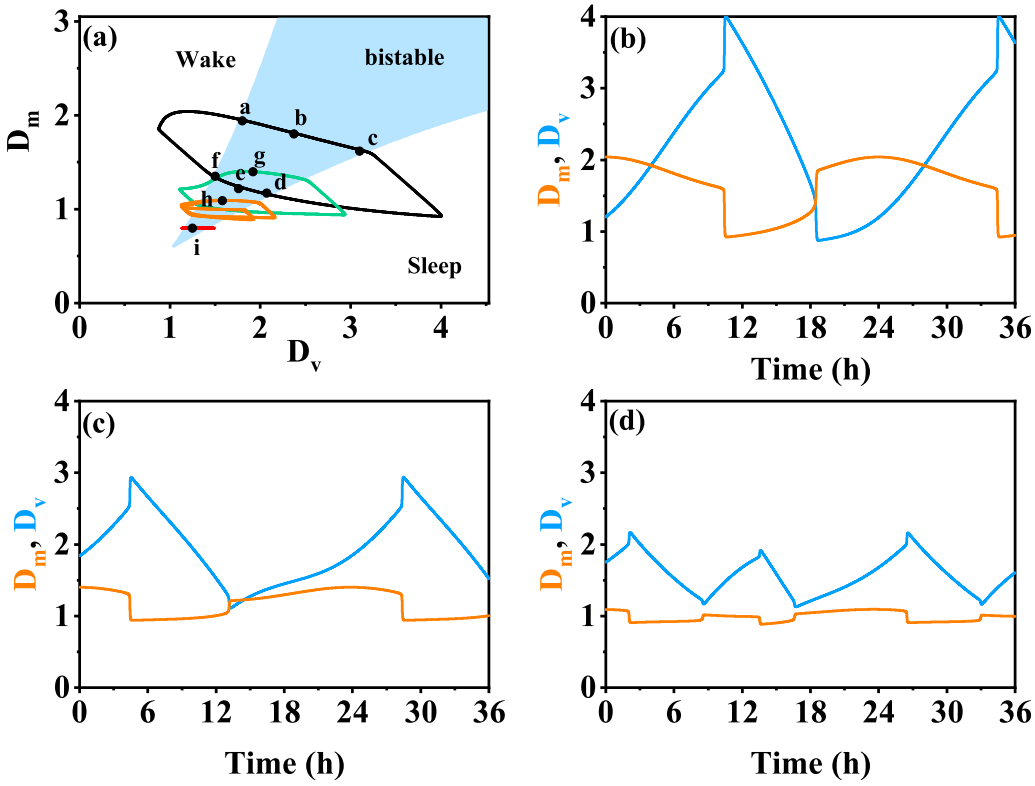

FIG. 3. (a) Phase diagram on the (D_v, D_m) plane for different dynamical regions. The bistable region is blue-shaded, and the wake and sleep regions are labeled. The trajectory loops for the different levels of Orx ($r_1 = 1.0, r_2 = 1.0$), ($r_1 = 0.5, r_2 = 0.5$), ($r_1 = 0.25, r_2 = 0.25$), and ($r_1 = 0.0, r_2 = 0.0$) are shown. (b)–(d) The time series of the dirve D_m (orange) and D_v (blue) for the different levels of Orx ($r_1 = 1.0, r_2 = 1.0$), ($r_1 = 0.5, r_2 = 0.5$), and ($r_1 = 0.25, r_2 = 0.25$), respectively.

falls asleep again, VLPO activates and suppresses Orx, resulting in a reduction in D_m and an increase in D_v, thus facilitating another bout of consolidated sleep.

Furthermore, upon comparing Figs. 3(b)–3(d), we observed that the oscillatory amplitudes of D_m and D_v decreased with decreasing levels of Orx, especially for D_m. As a result, the loop-like trajectory shifted towards the bottom-left corner and became smaller in the (D_v, D_m) plane. When Orx was completely removed from the model, the trajectory (the pink line) became even smaller, as depicted in Fig. 3(a). Therefore, we identified two key roles for Orx: (i) Orx excites the MA and inhibits the VLPO during wakefulness, thereby consolidating bouts of wake by increasing D_m and decreasing D_v. (ii) The reduced levels of Orx cause the oscillatory amplitudes of D_m and D_v to decrease, generating a bistable state in which both wake and sleep states are close to the saddle point.

C. The effect of Orx on thresholds for state transitions

To demonstrate the effects of Orx on the transition between wakefulness and sleep, Figs. 4(a)–4(d) provide time series for Q_m and Q_v with appropriate noise for $r_1 = r_2 = 1.0$, $r_1 = r_2 = 0.5$, $r_1 = r_2 = 0.25$, and $r_1 = r_2 = 0.0$, respectively. Figure 4(a) shows a simulated 36-h firing rate time series for normal wake/sleep, where noise does not influence the switch between wakefulness and sleep due to the consolidating role of Orx. When the level of Orx is appropriately reduced, as shown in Fig. 4(b), the switch between wakefulness and sleep is not influenced by noise. However, the duration of sleep is prolonged, indicating a weakened awakening function of Orx. Further reduction in the levels of Orx leads to an increased number of transitions between wakefulness and sleep, as induced by noise, as observed in Fig. 4(c) compared to Fig. 2(c_1). In the absence of Orx ($r_1 = r_2 = 0.0$), noise causes frequent state transitions, as shown in Fig. 4(d). The results suggest that the thresholds for state transitions decrease with decreasing levels of Orx.

To gain further insights into the influence of Orx levels on wake/sleep dynamics in a noisy environment, we analyzed two key factors: the average number of transitions (N) between wakefulness and sleep per day and the total sleep time. The results are illustrated in Fig. 5. In Fig. 5(a), it can be observed that the number of transitions (N) increases as the level (r) of Orx decreases below a critical value. This finding suggests that Orx plays a vital role in consolidating the cycle of wakefulness and sleep by maintaining a high threshold for state transitions. Additionally, Fig. 5(d) shows a slight increase in total sleep time per day.

To highlight the excitatory effect of Orx on the wake-promoting region (MA) and the inhibitory action of Orx on the

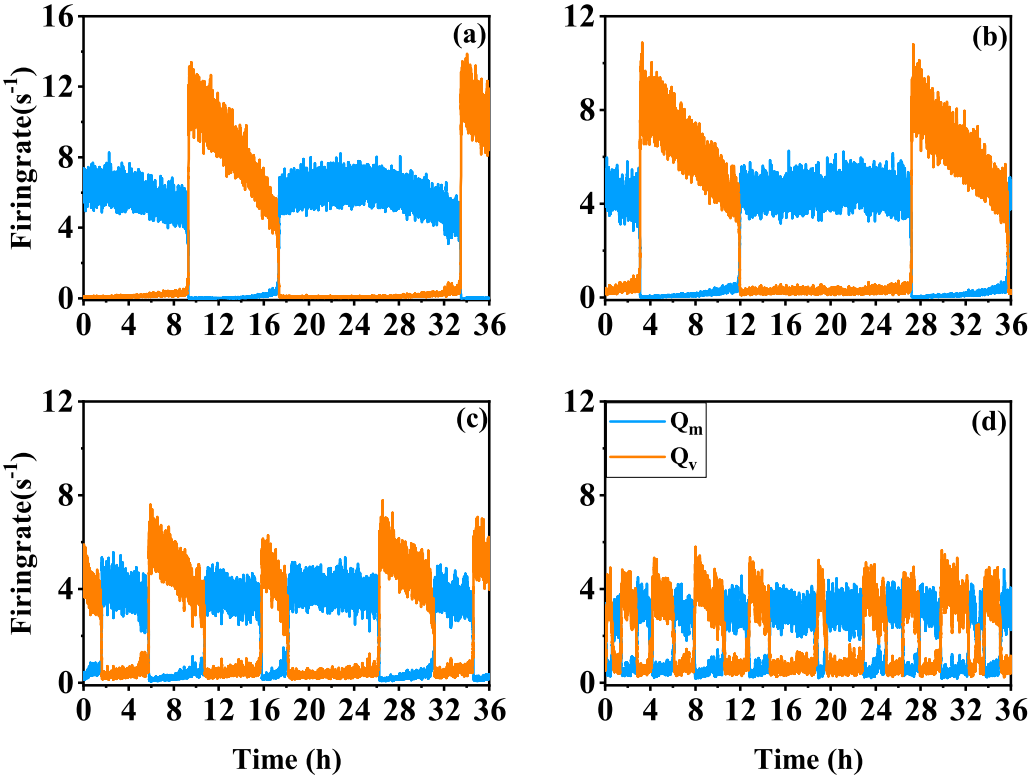

FIG. 4. (a)–(d) Time series for firing rates Q_m (blue) and Q_v (orange) in the noisy model for $(r_1 = 1.0, r_2 = 1.0)$, $(r_1 = 0.5, r_2 = 0.5)$, $(r_1 = 0.25, r_2 = 0.25)$, and $(r_1 = 0.0, r_2 = 0.0)$, respectively.

sleep-promoting region (VLPO), we examined the number of transitions for fixed values of $r_1 = 1.0$ (maintaining excitation) and $r_2 = 1.0$ (maintaining inhibition). Figures 5(b) and 5(c) depict the number of transitions under these conditions, while Figs. 5(e) and 5(f) display the corresponding total sleep time. Notably, when the excitation of Orx on MA is preserved and the inhibitory action of Orx on VLPO is varied [Fig. 5(e)], the number of transitions (N) remains constant at 1. On the other hand, N increases as r_1 decreases while maintaining the inhibitory action of Orx on VLPO. These findings suggest that the excitation of Orx on MA contributes to stabilizing the wakefulness and sleep cycle due to its excitatory effect.

Comparing Fig. 5(e) with Fig. 5(f), it is evident that the total sleep time exhibits a mild increase as r_2 decreases, while the total sleep time remains relatively constant as r_1 changes. These observations suggest that the inhibitory action of Orx on VLPO promotes awakening from sleep. Moreover, an interesting observation can be made by comparing Fig. 5(a) with Fig. 5(c): the number of transitions in the absence of both excitation and inhibition is significantly higher than when only excitation is absent. This finding indicates that the inhibition of Orx plays a crucial role in regulating wakefulness and sleep.

In summary, our findings demonstrate that Orx levels have a significant impact on wake/sleep dynamics. Decreasing Orx levels lead to an increased number of transitions between wakefulness and sleep, indicating the importance of Orx in maintaining a stable sleep-wake cycle. Furthermore, the excitatory effect of Orx on MA and the inhibitory action of Orx on VLPO contribute to the modulation of these transitions and the promotion of awakening from sleep. These results shed light on the intricate role of Orx in the regulation of sleep and wakefulness, emphasizing its significance in maintaining a balanced sleep-wake pattern.

D. Potential landscape and barrier

Although our previous data describe the dynamics of the new sleep model, we still lack an understanding of how Orx influences the threshold of transition between wakefulness and sleep, as well as the physical mechanisms underlying these transitions. To investigate these transitions in more detail, we applied the landscape and flux theory.[47] Equations (1a) and (1b) were simplified to the following equation:

$$\tau \frac{dx}{dt} = F(x) + \xi(t), \tag{7}$$

with $x = [V_m, V_v]$, $F(x) = [F_m(V_m, V_v), F_v(V_m, V_v)] = [-V_m + \nu_{mv}Q_v + D_m, -V_v + \nu_{vm}Q_m + D_v]$, and $\tau = [\tau_m, \tau_v]$. $\xi(t)$ represents independent Gaussian white noise with $\langle \xi_x(t) \rangle = 0$ and

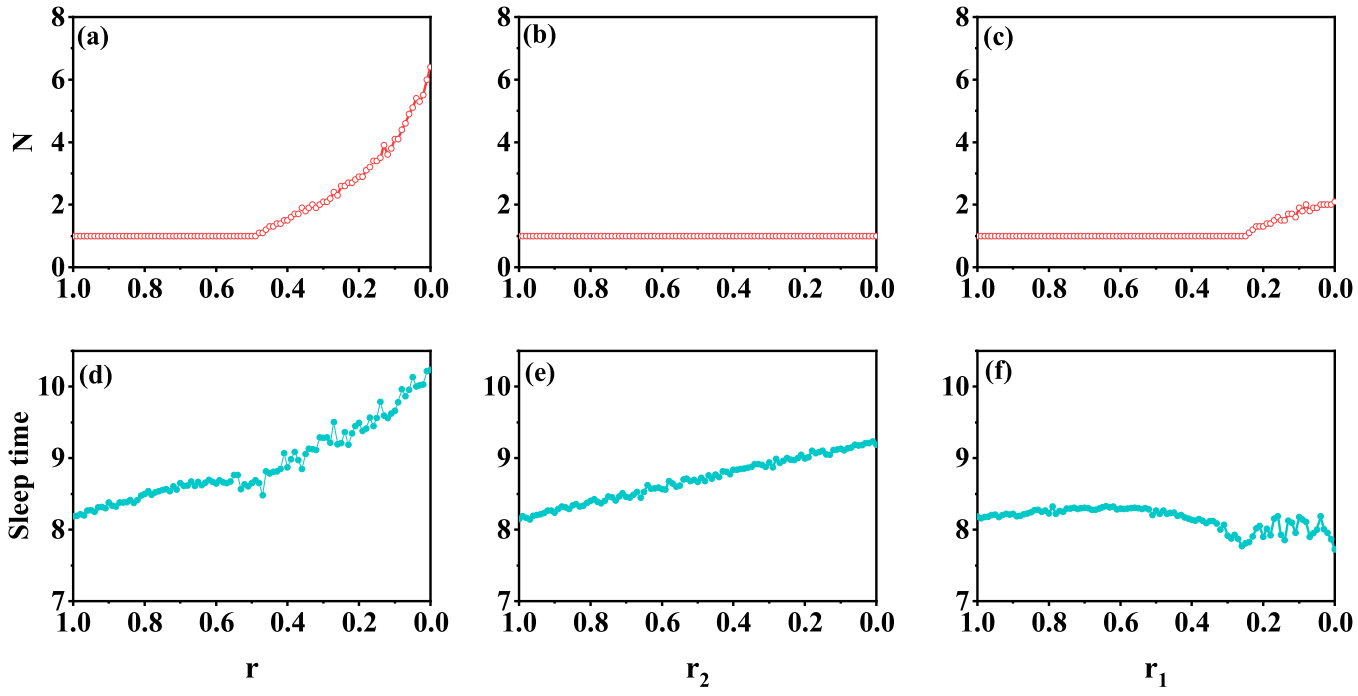

FIG. 5. The average number (N) of state transitions per day between wakefulness and sleep is plotted against the level of Orx in (a). The sleep process is simulated for ten days. (b) The number N is shown as a function of r_2 for $r_1 = 1.0$. (c) N is plotted against r_1 for $r_2 = 1.0$. The average total sleep time per day is computed and shown in (d)–(f), with the parameters remaining the same as in (a)–(c).

$\langle \xi_x(t)\xi_{x'}(t')\rangle = 2\sigma\delta(x-x')\delta(t-t')$, where σ denotes the noise strength.

In a stochastic system, the dynamical behavior is usually described by the probability distribution rather than the evolutionary trajectory of the system. The probability evolution of the stochastic differential equation satisfies

$$\frac{\partial P}{\partial t} = -\nabla \cdot J(x,t) = -\nabla \cdot [FP - \nabla \cdot (\sigma P)], \tag{8}$$

where J is the probability flux. This equation states that the rate of change of local probability is equal to the flux entering the system, based on the conservation law of probability. If the underlying system reaches a steady state, this equation can be written as

$$\frac{\partial P}{\partial t} = -\nabla \cdot J_{ss} = -\nabla \cdot [FP_{ss} - \nabla \cdot (\sigma P_{ss})] = 0. \tag{9}$$

There are two different solutions for $\nabla \cdot J_{ss} = 0$: $J_{ss} = 0$ and $J_{ss} \neq 0$. When $J_{ss} = 0$, it indicates a zero flux, leading to a state of detailed balance where there is no exchange of energy or information with the external environment in equilibrium. From Eq. (9), we found that $F(x) = -\sigma \frac{\partial U}{\partial x}$, where P_{ss} represents the probability distribution of the steady state, and the potential U is defined as

$$U = -\ln(P_{ss}). \tag{10}$$

In this case, it is evident that the equilibrium dynamics are solely controlled by the gradient of the potential or energy U. The equilibrium dynamics of the sleep system are similar to those of an electron moving in an electric field.

For $J_{ss} \neq 0$, we have $F(x) = -\sigma \frac{\partial U}{\partial x} + \frac{J_{ss}}{P_{ss}}$. The function $F(x)$ can be decomposed into the gradient of a potential $\left(-\sigma \frac{\partial U}{\partial x}\right)$ and a curl flow flux $\left(\frac{J_{ss}}{P_{ss}}\right)$.[47] Moreover, the detailed balance is broken due to the non-zero net flux, and the sleep system reaches a non-equilibrium state. The non-equilibrium dynamics of the sleep system, driven by the circadian and homeostatic drives, can be likened to electrons moving in both electric and magnetic fields.

Figure 6 depicts three-dimensional potential landscapes for different constant drives with a small noise strength. It is evident that (D_m, D_v) is situated near the boundary of node-saddle bifurcation, resulting in a weak bistable state characterized by a deep wake potential well and a shallow sleep potential well [Fig. 6(a)]. As D_m decreases and D_v increases, two basins of attraction emerge in the potential landscape, leading to a bistable state with both wake and sleep states. Moreover, the bistable state exhibits almost symmetrical characteristics [Fig. 6(b)]. With a further decrease in D_m and an increase in D_v, the second basin of attraction becomes deeper and more stable, while the wake state becomes unstable, ultimately transitioning the system into the sleep phase [Fig. 6(c)]. Conversely, the potential landscape undergoes opposite changes when D_m increases and D_v decreases, as depicted in Figs. 6(d)–6(f). Thus, the brain

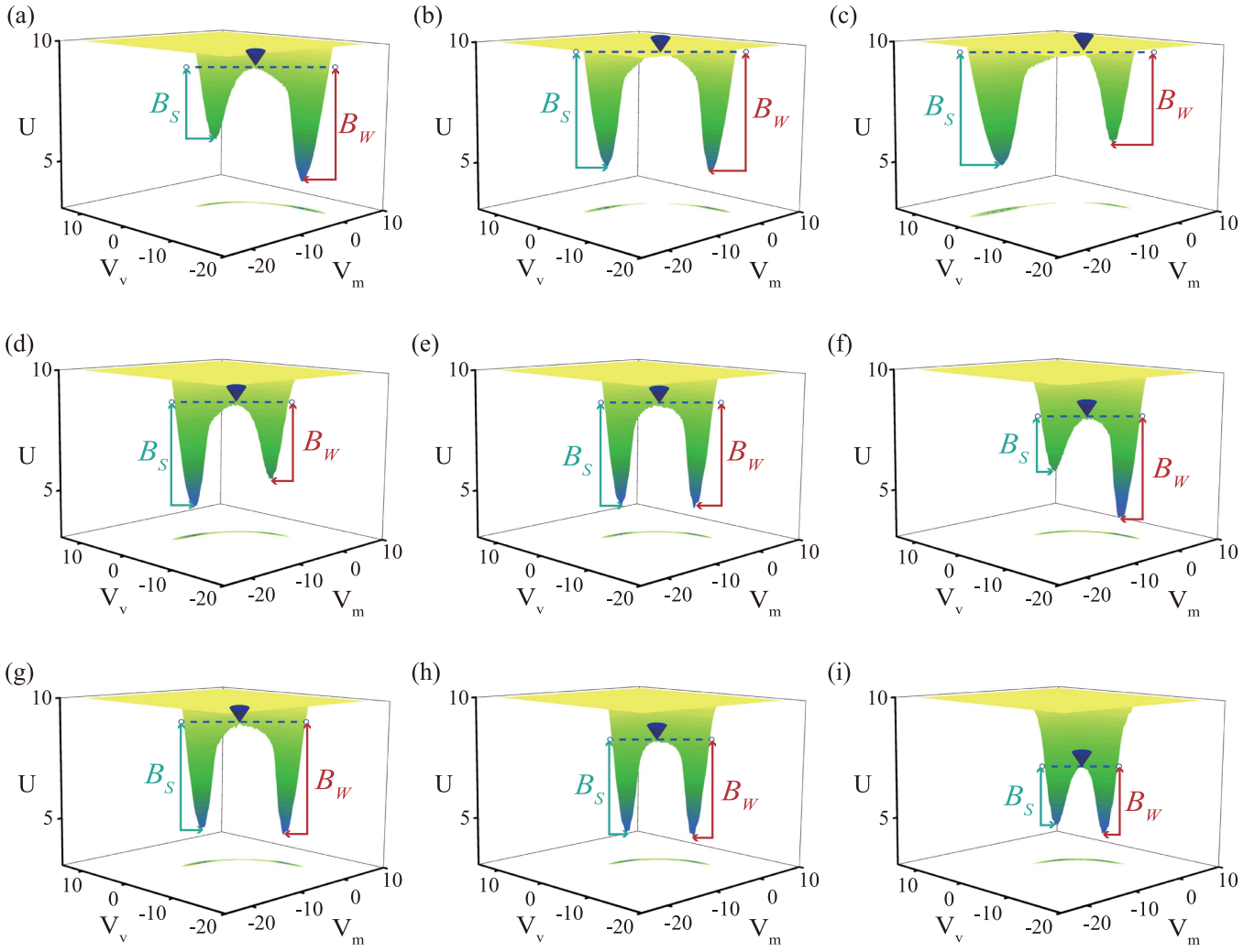

FIG. 6. (a)–(i) The three-dimensional landscape picture. (a) $(D_m, D_v) = (1.8, 1.94)$, (b) (2.37, 1.8), (c) (3.1, 1.62), (d) (2.07, 1.17), (e) (1.76, 1.22), (f) (1.5, 1.35), (g) (1.92, 1.4), (h) (1.58, 1.09), and (i) (1.25, 0.8). These parameters are denoted by filled circles in Fig. 3(a), respectively. B_s and B_w stand for the barriers of the stable sleep state and wake state, respectively.

achieves the transition between wakefulness and sleep by traversing different barrier heights through adjustments in D_m and D_v, combining interactions among the homeostatic process, Orx, and the circadian drive.

To examine the impact of Orx levels on thresholds for state transitions, we selected specific parameters (D_m, D_v) situated in different loops associated with varying levels of Orx. Comparing Figs. 6(b), 6(g), 6(h), and 6(i), we observed four basins of attraction with varying depths. As both D_m and D_v decreased, the depths of the wake and sleep state valleys visibly diminished, indicating a gradual destabilization of the basin of attraction. The barrier height of the bistable state between wakefulness and sleep decreased as D_m and D_v decreased. Consequently, a reduction in Orx levels leads the brain to a bistable state with a lower threshold, thus inducing narcolepsy characterized by frequent state transitions triggered by external environmental disturbances. It is important to emphasize that our primary objective was to illustrate the physical mechanisms and qualitative behavior of our model as Orx levels fluctuate. What is more, the quantitative values predicted in this study could be fitted to specific clinical datasets in future research.

IV. CONCLUSIONS

In this study, we developed a mathematical model of wakefulness and sleep regulated by Orx based on new experimental findings, which revealed an indirect inhibitory effect of sleep-promoting neurons in the ventrolateral preoptic nucleus. Using a sleep model as the foundation, we constructed a neural circuit incorporating

physiological knowledge and provided a clear understanding of the physical mechanisms and quantification of narcolepsy, a disorder characterized by instability in the arousal state due to the loss of Orx. The model exhibited mutual inhibitions and featured two "flip-flop" switches between wakefulness and sleep, with each group of neurons indirectly reinforcing its own firing. Only one neuronal population could be active at a time, leading to rapid transitions between states.

Our model successfully reproduced the dynamic behavior of normal sleep, by taking into account the influence of circadian drive and homeostatic processes under appropriate physiological parameters. Additionally, it provided an explanation for various features observed in narcolepsy. We elucidated the underlying mechanisms of normal sleep through net drive loops in the (D_m, D_v) plane. Importantly, we identified distinct effects of Orx, resulting from its excitatory impact on the monoaminergic (MA) group and its inhibitory action on the ventrolateral preoptic nucleus (VLPO). The excitation of Orx on MA played a crucial role in stabilizing the wake/sleep cycle by maintaining wakefulness, while the inhibitory action of Orx on VLPO contributed to the transition from sleep to wakefulness.

Furthermore, we demonstrated the sleep fragmentation characteristics of narcolepsy by simulating a reduction in Orx levels within the sleep model. A decreased level of Orx shifted the system to a bistable state with a lower threshold, leading to fragmented wake/sleep patterns resembling those observed in narcolepsy, characterized by frequent state transitions.

To elucidate the physical mechanism by which the loss of Orx induces fragmented sleep, we conducted further investigations into the global nature of the sleep system using the theory of potential landscapes. Our findings revealed that the sleep system can be effectively characterized by the topography of its landscape. The barrier height of the potential landscape served as a quantitative indicator of stability. We observed that the transitions between wakefulness and sleep in the brain occur through the traversal of different barrier heights, achieved by modulating the parameters D_m and D_v, by considering the interactions among the homeostatic process, Orx levels, and the circadian drive. When the level of Orx is reduced, leading to a decrease in D_m and D_v, the system enters a bistable state with an extremely low threshold. Consequently, fragmented sleep accompanied by frequent state transitions arises due to the susceptibility of the system to external environmental disturbances. By examining brain states through the lens of potential landscapes, we can gain a deeper understanding of the underlying physical processes involved in the transitions between different brain states.

Our research presents a novel sleep model that significantly enhances our comprehension of the regulatory role of Orx in sleep, particularly in relation to fragmented sleep with frequent transitions. Although the exact action network of Orx is not fully elucidated, our simplified model in this paper successfully demonstrates that normal sleep and the key characteristic of narcolepsy can be attributed to the loss of Orx. Furthermore, we have identified distinct effects of Orx on the regulation of sleep architecture, which are mediated by the excitation of Orx on MA and the inhibition of Orx on VLPO. Developing a more realistic and comprehensive model has the potential to provide deeper insights into the biological functions of the brain and further advance our understanding in this field.

The Orx system plays a crucial role in regulating wakefulness and sleep in mammals. Orx neurons are involved in promoting arousal and maintaining wakefulness. The loss or dysfunction of Orx neurons has been linked to sleep disorders such as narcolepsy, characterized by excessive daytime sleepiness and sudden loss of muscle tone (cataplexy).[48,49] Research has shown that Orx acts as a key modulator of the wake/sleep cycle by influencing various brain regions involved in sleep regulation.[50] Additionally, Orx is involved in regulating rapid eye movement (REM) sleep, a phase associated with vivid dreaming and important physiological functions. Orx neurons inhibit REM sleep-promoting regions, such as the ventrolateral periaqueductal gray (vlPAG), and suppress muscle atonia during REM sleep.[51] Understanding the role of Orx in wake/sleep regulation has significant implications for the development of therapies targeting sleep disorders. Manipulating the Orx system through Orx receptor agonists or antagonists has shown promising results in the treatment of narcolepsy and other sleep disorders.[5]

ACKNOWLEDGMENTS

This work was supported by the Ministry of Science and Technology of the People's Republic of China (STI2030-Major Projects 2021ZD0201900), the National Natural Science Foundation of China (NNSFC) under Grant Nos. 12175242, 12075089, and 12090052, the Wenzhou Key Laboratory of Biophysics under Grant No. WIUCASSWWL22004, and the Jiaxing Public Welfare Project under No. 2022AD10014.

AUTHOR DECLARATIONS

Conflict of Interest

The authors declared that they have no conflicts to disclose.

Author Contributions

Chenggui Yao: Conceptualization (equal); Methodology (equal); Validation (equal); Writing – original draft (equal). **Fei Xu:** Conceptualization (equal); Formal analysis (equal); Software (equal); Validation (equal). **Xiangdong Tang:** Conceptualization (equal); Investigation (equal); Validation (equal). **Wei Zou:** Conceptualization (equal); Validation (equal); Writing – review & editing (equal). **Dongping Yang:** Conceptualization (equal); Validation (equal); Writing – original draft (equal). **Jianwei Shuai:** Conceptualization (equal); Supervision (equal).

DATA AVAILABILITY

The data that support the findings of this study are available from the corresponding authors upon reasonable request.

REFERENCES

[1]T. Sakurai, A. Amemiya, M. Ishii, I. Matsuzaki, R. M. Chemelli, H. Tanaka, S. C. Williams, J. A. Richardson, G. P. Kozlowski, S. Wilson, J. R. S. Arch, R. E. Buckingham, A. C. Haynes, S. A. Carr, R. S. Annan, D. E. McNulty, W.-S. Liu, J. A. Terrett, N. A. Elshourbagy, D. J. Bergsma, and M. Yanagisawa, Cell **92**, 573 (1998).
[2]L. de Lecea, T. S. Kilduff, C. Peyron, X.-B. Gao, P. E. Foye, P. E. Danielson, C. Fukuhara, E. L. F. Battenberg, V. T. Gautvik, F. S. Bartlett, W. N. Frankel, A. N.

van den Pol, F. E. Bloom, K. M. Gautvik, and J. G. Sutcliffe, Proc. Natl. Acad. Sci. U.S.A. **95**, 322 (1998).
[3]S. B. Li and L. de Lecea, Neuropharmacology **167**, 107993 (2020).
[4]T. Sakurai, M. Mieda, and N. Tsujino, Ann. N. Y. Acad. Sci. **1200**, 149 (2010).
[5]T. Sakurai, Nat. Rev. Neurosci. **15**, 719 (2014).
[6]T. Sakurai, Nat. Rev. Neurosci. **8**, 171 (2007).
[7]J. P. Kukkonen, T. Holmqvist, S. Ammoun, and K. E. O. Akerman, Am. J. Physiol. Cell Physiol. **283**, 1567 (2002).
[8]M. Mieda, S. C. Williams, C. M. Sinton, J. A. Richardson, T. Sakurai, and M. Yanagisawa, J. Neurosci. **24**, 10493 (2004).
[9]T. E. Scammell and C. B. Saper, Nat. Neurosci. **8**, 1286 (2005).
[10]T. Mochizuki, A. Crocker, S. McCormack, M. Yanagisawa, T. Sakurai, and T. E. Scammell, J. Neurosci. **24**, 6291 (2004).
[11]T. C. Thannickal, R. Y. Moore, R. Nienhuis, L. Ramanathan, S. Gulyani, M. Aldrich, M. Cornford, and J. M. Siegel, Neuron **27**, 469 (2000).
[12]M. H. Silber, L. E. Krahn, E. J. Olson, and S. Pankratz, Sleep **25**, 197 (2002).
[13]Y. Shi, R. Ren, F. Lei, Y. Zhang, M. V. Vitiello, and X. Tang, Front. Neurosci. **16**, 1045934 (2022).
[14]J. W. Shuai, Front. Neurosci. **17**, 1176932 (2023).
[15]X. X. Wu, C. G. Yao, and J. W. Shuai, Sci. Rep. **5**, 7684 (2015).
[16]X. Zhang, J. W. Kantelhardt, X. S. Dong, D. Krefting, J. Li, H. Yan, F. Pillmann, I. Fietze, T. Penzel, L. Zhao, and F. Han, Sleep **40**, 2 (2017).
[17]B. R. Kornum, S. Knudsen, H. M. Ollila, F. Pizza, P. J. Jennum, Y. Dauvilliers, and S. Overeem, Nat. Rev. Dis. Primers **3**, 16100 (2017).
[18]C. Alexandre, M. L. Andermann, and T. E. Scammell, Curr. Opin. Neurobiol. **23**, 752 (2003).
[19]B. D. Fulcher, A. J. K. Phillips, S. Postnova, and P. A. Robinson, PLoS One **9**, e91982 (2014).
[20]R. D. De Luca, S. Nardone, K. P. Grace, A. Venner, M. Cristofolini, S. S. Bandaru, L. T. Sohn, D. Kong, T. Mochizuki, B. Viberti, L. Zhu, A. Zito, T. E. Scammell, C. B. Saper, B. B. Lowell, P. M. Fuller, and E. Arrigoni, Nat. Commun. **13**, 4163 (2022).
[21]C. B. Saper, T. E. Scammell, and J. Lu, Nature **437**, 1257 (2005).
[22]D. Pimentel, J. M. Donlea, C. B. Talbot, S. M. Song, A. J. F. Thurston, and G. Miesenbock, Nature **536**, 333 (2016).
[23]E. F. Pace-Schott and J. A. Hobson, Nat. Rev. Neurosci. **3**, 591 (2002).
[24]A. J. K. Phillips and P. A. Robinson, J. Biol. Rhythms **22**, 167 (2007).
[25]A. J. K. Phillips and P. A. Robinson, J. Theor. Biol. **255**, 413 (2008).
[26]D. P. Yang, L. McKenzie-Sell, A. Karanjai, and P. A. Robinson, Phys. Rev. E **94**, 022412 (2016).
[27]R. E. Brown, R. Basheer, J. T. McKenna, R. E. Strecker, and R. W. McCarley, Physiol. Rev. **92**, 1087 (2012).
[28]C. B. Saper, P. M. Fuller, N. P. Pedersen, J. Lu, and T. E. Scammell, Neuron **68**, 1023 (2010).
[29]T. E. Scammell, E. Arrigoni, and J. O. Lipton, Neuron **93**, 747 (2017).
[30]E. C. Harding, X. Yu, A. Miao, N. Andrews, Y. Ma, Z. Ye, L. Lignos, G. Miracca, W. Ba, R. Yustos, A. L. Vyssotski, W. Wisden, and N. P. Franks, Curr. Biol. **28**, 2263 (2018).
[31]C. Anaclet, L. Ferrari, E. Arrigoni, C. E. Bass, C. B. Saper, J. Lu, and P. M. Fuller, Nat. Neurosci. **17**, 1217 (2014).
[32]Y. Hayashi, M. Kashiwagi, K. Yasuda, R. Ando, and M. Kanuka, Science **350**, 957 (2015).
[33]A. A. Borbely, Hum. Neurobiol. **1**, 195 (1982).
[34]J. M. Krueger, D. M. Rector, S. Roy, H. P. A. Van Dongen, G. Belenky, and J. Panksepp, Nat. Rev. Neurosci. **9**, 910 (2008).
[35]A. J. K. Phillips, B. D. Fulcher, P. A. Robinson, and E. B. Klerman, PLoS Comput. Biol. **9**, e1003213 (2013).
[36]P. A. Robinson, A. J. K. Phillips, B. D. Fulcher, M. Puckeridge, and J. A. Roberts, Philos. Trans. A: Math. Phys. Eng. Sci. **369**, 3840 (2011).
[37]S. Daan, D. G. M. Beersma, and A. A. Borbely, Am. J. Physiol. Regul. Integr. Comp. Physiol. **246**, 161 (1984).
[38]M. Nakao, A. Karashima, and N. Katayama, Cell Mol. Life Sci. **64**, 1236 (2007).
[39]A. A. Borbely and P. Achermann, J. Biol. Rhythms **14**, 559 (1999).
[40]C. B. Saper, T. C. Chou, and T. E. Scammell, Trends Neurosci. **24**, 726 (2001).
[41]T. Gallopin, P. Fort, E. Eggermann, B. Cauli, P. H. Luppi, J. Rossier, E. Audinat, M. Mühlethaler, and M. Serafin, Nature **404**, 992 (2000).
[42]C. B.Saper, G. Cano, and T. E. Scammell, J. Comp. Neurol. **493**, 92 (2005).
[43]J. J. Gooley, A. Schomer, and C. B. Saper, Nat. Neurosci. **9**, 398 (2006).
[44]C. B. Saper, T. C. Chou, and T. E. Scammell, Trends Neurosci. **24**, 726 (2001).
[45]S. Kantor, T. Mochizuki, A. M. Janisiewicz, E. Clark, S. Nishino, and T. E. Scammell, Sleep **32**, 1127 (2009).
[46]J. Lu, M. Greco, P. Shiromani, and C. B. Saper, J. Neurosci. **20**, 3830 (2000).
[47]L. Xu, D. Patterson, A. C. Staver, and J. Wang, Proc. Natl. Acad. Sci. U.S.A. **118**, e2103779118 (2021).
[48]S. Nishino and E. Mignot, Prog. Neurobiol. **52**, 27 (1997).
[49]R. M. Chemelli, J. T. Willie, C. M. Sinto, J. K. Elmquist, T. Scammell, C. Lee, J. A. Richardson, S. C. Williams, Y. Xiong, Y. Kisanuki, T. E. Fitch, M. Nakazato, R. E. Hammer, C. B. Saper, and M. Yanagisawa, Cell **98**, 437 (1999).
[50]C. Peyron, D. K. Tighe, A. N. van den Pol, L. de Lecea, H. C. Heller, J. G. Sutcliffe, and T. S. Kilduff, J. Neurosci. **18**, 9996 (1998).
[51]H. J. Lee, L. Y. Chang, Y. C. Ho, S.-F. Teng, L.-L. Hwang, K. Mackie, and L.-C. Chiou, Neuropharmacology **105**, 577 (2016).